Seasonal and Diurnal Variations in Rainfall Characteristics over the Tropical Asian Monsoon Region Using TRMM-PR Data

Hiroshi G. Takahashi[1, 2]

[1]*Department of Geography, Tokyo Metropolitan University, Hachioji, Japan*
[2]*Japan Agency for Marine-Earth Science and Technology, Yokohama, Japan*

Abstract

Seasonal and diurnal rainfall characteristics, including the rainfall amount (RA), rainfall frequency (RF), and rainfall intensity (RI), were investigated over the tropical Asian monsoon region using Tropical Rainfall Measuring Mission Precipitation Radar (TRMM-PR) data. The results showed that the number of hours of high RF varied seasonally over land, although the diurnal peaks were mostly unchanged. Over Indochina, precipitation ended in the evening in April and May when the RA was low, whereas precipitation lasted until early morning from July to September when the RA was high. The seasonal changes in RF likely contributed to the changes in RA over land. Additionally, RI had two seasonal peaks occurring at the beginning and end of the summer monsoon over land regions; thus, RI was strongest during the two transition seasons. In contrast, both RF and RI had a single seasonal peak over the ocean.

(**Citation**: Takahashi, H. G., 2016: Seasonal and diurnal variations in rainfall characteristics over the tropical Asian monsoon region using TRMM-PR data. *SOLA*, **12A**, 22−27, doi:10.2151/sola.12A-005.)

1. Introduction

The diurnal precipitation variation over the tropical Asian summer monsoon region is climatologically dominant. Precipitation activity over land is dominant during the day, whereas over the coastal ocean precipitation is active until midnight and in the morning. The Tropical Rainfall Measuring Mission Precipitation Radar (TRMM-PR), a precipitation radar system mounted on the non-sun-synchronous TRMM satellite, demonstrates a very clear diurnal rainfall cycle over the entire tropical region (e.g., Hirose et al. 2008). In addition to TRMM results, many studies have investigated the diurnal rainfall variation over Southeast Asia using rain gauge and ground-installed radar (Ohsawa et al. 2000; Okumura et al. 2003; Satomura et al. 2011), and numerical simulations (Satomura 2000; Kataoka and Satomura 2005; Takahashi et al. 2010b; Takahashi et al. 2012).

Long-term observation by long-lasting TRMM-PR permits climatological examination of the diurnal rainfall cycle over the tropical regions, including areas with sparse observation networks. However, most studies have investigated the annual or seasonal mean diurnal rainfall cycles. This may be due to the less frequent sampling of TRMM-PR observations than conventional global precipitation datasets based on infrared images. Additionally, despite the recent launch of the Global Precipitation Measurement (GPM) satellite, GPM-Dual-frequency Precipitation Radar (GPM-DPR) observations are only available for a few years, and there is insufficient data to analyze the seasonal and interannual variation of diurnal rainfall cycles. Thus, we should use TRMM-PR data to understand the seasonal and interannual variations in diurnal rainfall cycles.

The seasonal march of rainfall and its interannual variation dominate the tropical Asian monsoon region (e.g., Wang 2006). Several previous studies have focused on seasonal change of diurnal convective systems over Malaysia and Japan (Oki and Mushiake 1994), the Tibetan Plateau (e.g., Fujinami and Yasunari 2001), South Asia (Kodama et al. 2005; Romatschke et al. 2010; Romatschke and Houze 2011a, 2011b), and some tropical regions (e.g., Biasutti et al. 2012). The studies in South Asia found that convective rainfall systems are dominant in the pre-monsoon season. In addition, the systems become more stratiform from the pre-monsoon to monsoon seasons. However, the seasonal variation in the diurnal precipitation cycle is not fully understood. It is quite possible that diurnal precipitation variation changes with the seasonal march of the Asian monsoon system. Therefore, this study focused on the seasonal variation in diurnal precipitation variation over the Asian monsoon region.

Rainfall characteristics, such as rainfall amount (RA), rainfall frequency (RF), and rainfall intensity (RI), have become increasingly important due to their changes in response to a warmer climate. For example, it is well known that the global warming can induce an increase in precipitation amount and a decrease in weaker precipitation events (e.g., IPCC 2013). Relatively few studies have addressed seasonal and diurnal variations of precipitation characteristics (e.g., Takahashi et al. 2010a; Takahashi 2010).

The purpose of this study was to describe the seasonal and diurnal rainfall variations from the long-term TRMM-PR observations over the Asian monsoon region. We also discussed the differences in the seasonal and diurnal variations of rainfall characteristics between land and ocean.

2. Datasets and methods

2.1 Datasets

We used TRMM-PR 3G68 (ver. 7), a grid version of the TRMM-PR rainfall 2A25 product (Iguchi et al., 2000, 2009). Hereafter, we refer to these rainfall data as TRMM-PR. The TRMM3G68 product includes the grid-averaged hourly rainfall rate (RR), the number of precipitation pixels ($N_{total\ precip}$), and the number of observation pixels ($N_{total\ obs}$). The footprints have an approximately 5-km diameter. The TRMM satellite was boosted from 350 to 403 km in August 2001, which increased the footprint for TRMM-PR from 4.3- to 5-km diameter (Shimizu et al. 2009). The statistics of these data were archived at a 0.25 × 0.25-degree grid resolution within the tropics and subtropics (approximately 36.5°S−36.5°N). The 15 years of TRMM-PR observations spanned the period 1998−2012. Over the Asian monsoon region, diurnal precipitation variation is quite predominant. In all of the figures shown here, we use a local solar time for the respective regions, which is shown in the figure legends.

2.2 Definition of rainfall characteristics

To understand the rainfall characteristics, we defined RA, RF and RI. Three parameters were calculated from the TRMM-PR product at each hourly time slot. The RA was defined as the total rainfall amount for 15 years divided by the total number of observations ($RA = \Sigma RR/N_{total\ obs}$). The RF, expressed as a percentage, was determined by dividing the number of surface precipitation pixels by the total number of observation pixels; precipitation was confirmed when the 2A25 algorithm indicated the existence of near-surface rainfall ($RF = N_{total\ precip}/N_{total\ obs}$). The RI was

Corresponding author: Hiroshi G. Takahashi, Department of Geography, Tokyo Metropolitan University, Hachioji, Tokyo, 192-0397, Japan. E-mail: hiroshi3@tmu.ac.jp.

calculated as the RA divided by the RF ($RI = RA/RF$). The RF may be underestimated because the limit of rainfall detection by TRMM-PR is approximately 0.5 mm h^{-1}; thus, weaker precipitation may not be detected.

3. Results

3.1 Rainfall characteristics over land

3.1.1 RF over land

We investigated seasonal and diurnal variations in precipitation characteristics over the tropical Asian monsoon regions. To understand the differences in the seasonal and diurnal variations in precipitation characteristics between land and ocean, we selected six target regions (Fig. 1): the Indian Subcontinent (77°E–82°E, 15°N–19°N), Indochina Peninsula (100°E–105°E, 15°N–20°N), Bangladesh Plain (88°E–93°E, 23°N–27°N), Bay of Bengal (85°E–95°E, 12°N–18°N), South China Sea (110°E–120°E, 12°N–18°N), and western North Pacific (128°E–138°E, 8°N–14°N). These target regions were selected based on major latent heat source regions of the Asian monsoon, which are over and around the Bay of Bengal and the western North Pacific (e.g., Wang and Fan 1999).

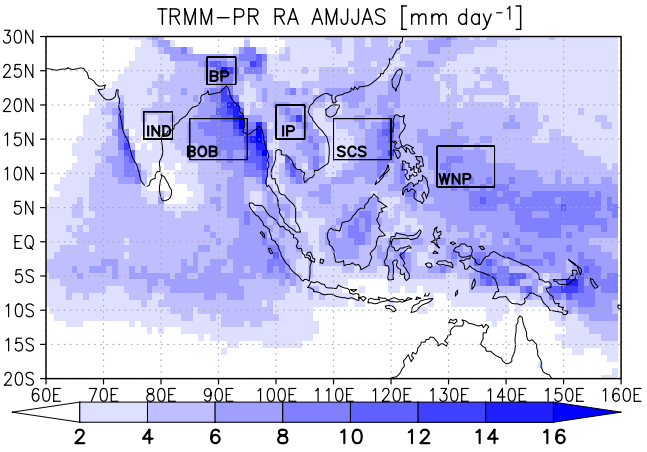

Fig. 1. A 15-year climatology of rainfall amount (RA) from April to September over the tropical Asian monsoon region observed by Tropical Rainfall Measuring Mission Precipitation Radar (TRMM-PR). The spatial grid scale was converted on a 1° × 1° grid. The unit is mm day^{-1}. The boxes indicate the six selected regions for detailed investigation. The abbreviated expressions for the Indian Subcontinent, Indochina Peninsula, Bangladesh Plain, Bay of Bengal, South China Sea, and western North Pacific are IND, IP, BP, BOB, SCS, and WNP, respectively.

In the Indian Subcontinent, a high RF was observed during the major rainy season (Fig. 2a), although the peak was indistinctly observed in the latter half of the season. There were more hours with a high RF in August than in June. The seasonal changes in RF were similar to those in RA, which implies that they probably contributed to those in RA.

Seasonal peaks in the RF were observed from May to September over the Indochina Peninsula (Fig. 2b), which is the major rainy season. In June, the RF showed a small dip, which was consistent with the climatological monsoon break over the Indochina Peninsula (Takahashi and Yasunari 2006). The seasonal variation in diurnal RF showed an increase in the frequency of hours with a high RF within the day, with seasonal march. In pre-monsoon periods and at the beginning of the rainy season, specifically from April to May, RF was higher during the early afternoon to evening, whereas in the second half of the rainy season, during July and August, high RF was also observed at early morning.

Similar to the other land regions, a single seasonal peak in RF was observed over the Bangladesh Plain (Fig. 2c). Again, the daily-accumulated RA was associated with the number of hours with a high RF. A high RF was observed in the evening and early morning. The rainfall activities in the evening and early morning may differ, with daytime precipitation over the whole plain and nocturnal precipitation over the Meghalaya Hills (e.g., Hirose and Nakamura 2005).

3.1.2 RI over land

Over the Indian Subcontinent, seasonal peaks in RI were observed in and around April and September (Fig. 3a), which is the timing of the beginning and end of the monsoon season, respectively. This indicates that the RI was strongest during the transition seasons between rainy and dry seasons. The diurnal peaks in RI occurred in the early afternoon.

Seasonal peaks in RI were observed over the Indochina Peninsula in and around April and September (Fig. 3b), which are the transition periods between the rainy and dry seasons. A diurnal peak in RI occurred in the early afternoon. However, RI was not weak during the nighttime.

A noticeable seasonal peak in RI was found over the Bangladesh Plain in and around April (Fig. 3c). A minor seasonal peak in RI was observed in September. In terms of diurnal RI variation, stronger precipitation occurred over this region in the early afternoon and early morning. As mentioned for RF, these two peaks were composed of daytime precipitation over the whole plain and nocturnal precipitation over the Meghalaya Hills. In addition, this stronger RI in the pre-monsoon season may be associated with severe local storms over Bangladesh (e.g., Yamane et al. 2013).

These characteristics are partly consistent with those observed by Kodama et al. (2005), who showed that convective-type precipitation is dominant around Bangladesh in the pre-monsoon

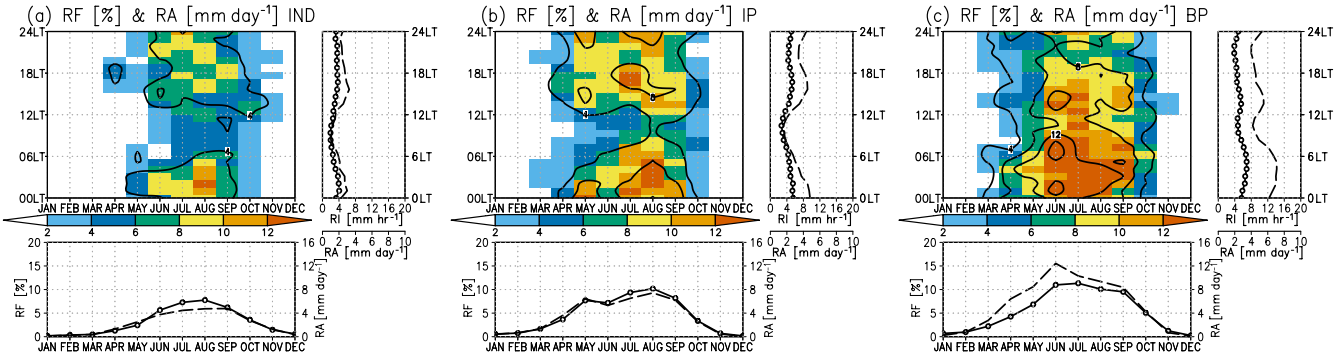

Fig. 2. Seasonal and diurnal cross-section of rainfall frequency (RF; color) and rainfall amount (RA: contours of 4, 8, 12, and 16 mm day^{-1}) over (a) the Indian Subcontinent (77°E–82°E, 15°N–19°N), (b) Indochina Peninsula (100°E–105°E, 15°N–20°N), and (c) Bangladesh Plain (88°E–93°E, 23°N–27°N). Local solar time is set to (a) +5 hours, (b) +7 hours, and (c) +6 hours to UTC. RF is defined in Section 2.2. For each region, the bottom panel indicates the seasonal march of daily RF (solid line with open circle) and RA (short dashed line). The right panel shows the annual mean diurnal cycles of RF (solid line with open circle) and RA (short dashed line). For smoothing, a 3-hourly running mean was applied to ensure less sampling up in the diurnal direction. The unit of RF (RA) is percent (mm day^{-1}).

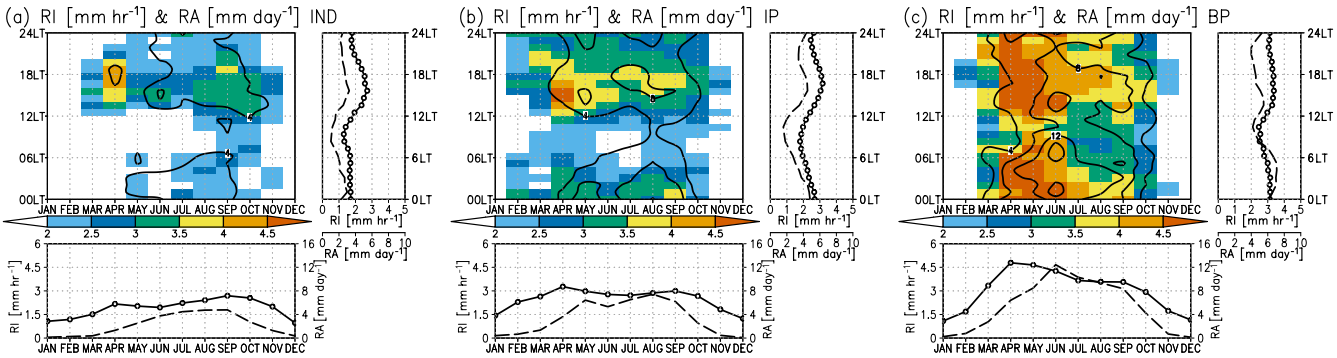

Fig. 3. Same as Fig. 2 but for RI. RA is also plotted in this figure. In the cross-section, color denotes RI and contours (4, 8, 12, and 16 mm day^{-1}) indicate RA. For each region, the bottom panel indicates the seasonal march of daily RI (solid line with open circle) and RA (short dashed line). The right panel shows the annual mean diurnal cycles of RI (solid line with open circle) and RA (short dashed line). The unit of RI (RA) is mm h^{-1} (mm day^{-1}).

season. However, heavy RI was also observed at the end of the rainy season, although there were regional differences in seasonal RI changes. A heavy RI was observed in the transition seasons between the dry and wet seasons.

3.2 Precipitation characteristics over the ocean

3.2.1 RF over the ocean

To understand the difference in seasonal and diurnal variations of rainfall characteristics between land and ocean, we also examined the rainfall characteristics over the Bay of Bengal, South China Sea, and western North Pacific (Fig. 1).

A single seasonal peak was observed during the major rainy season from June to September over the Bay of Bengal. Diurnal peaks in RF occurred from the early morning to the early afternoon from June to September, over the Bay of Bengal (Fig. 4a). The diurnal minimum was observed during evening hours when the diurnal precipitation peak occurred over the land regions. Over the South China Sea, a single seasonal peak was observed during the major rainy season from June to September (Fig. 4b). Diurnal peaks in RF were not clear except in the morning. Similar to the other ocean regions, a single seasonal RF peak occurred in August over the western North Pacific (Fig. 4c).

These results indicate that the seasonal variation in RF was similar to that of the land region. However, the seasonal variation of diurnal RF variations within the rainy season was less clear than in the land regions. In addition, the absolute values of RF over the ocean were slightly larger than those of the land regions.

3.2.2 RI over the ocean

There were clear seasonal variations of RI over the Bay of Bengal. A higher RI was observed throughout the rainy season. In terms of diurnal RI variation, precipitation was the strongest during the late morning and early afternoon hours (Fig. 5a).

The seasonal and diurnal variations of RI over the South China Sea were weaker than those over land regions (Fig. 5b). A relatively higher RI was observed from July to October. The sea-

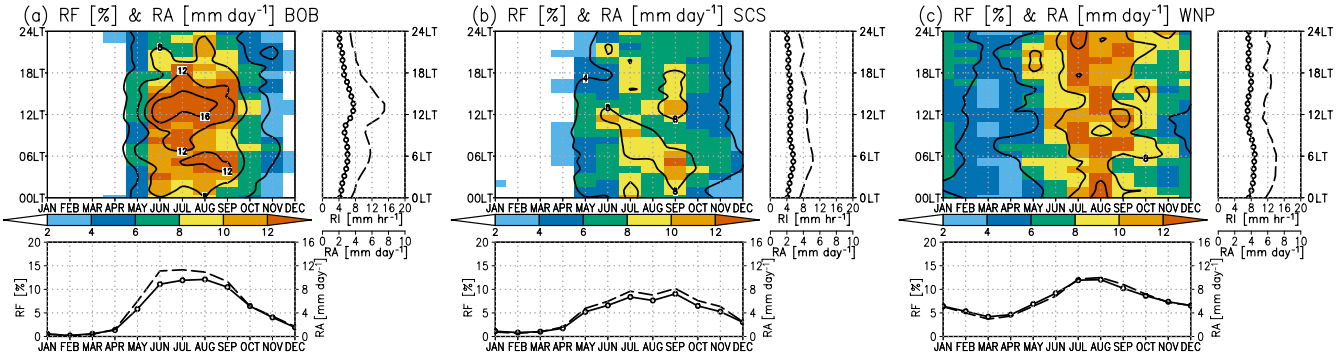

Fig. 4. Same as Fig. 2 but for oceanic regions, (a) Bay of Bengal (85°E−95°E, 12°N−18°N), (b)South China Sea (110°E−120°E, 12°N−18°N), and (c) western North Pacific (128°E−138°E, 8°N−14°N). Local solar time is set to (a) +6 hours, (b) +8 hours, and (c) +9 hours to UTC.

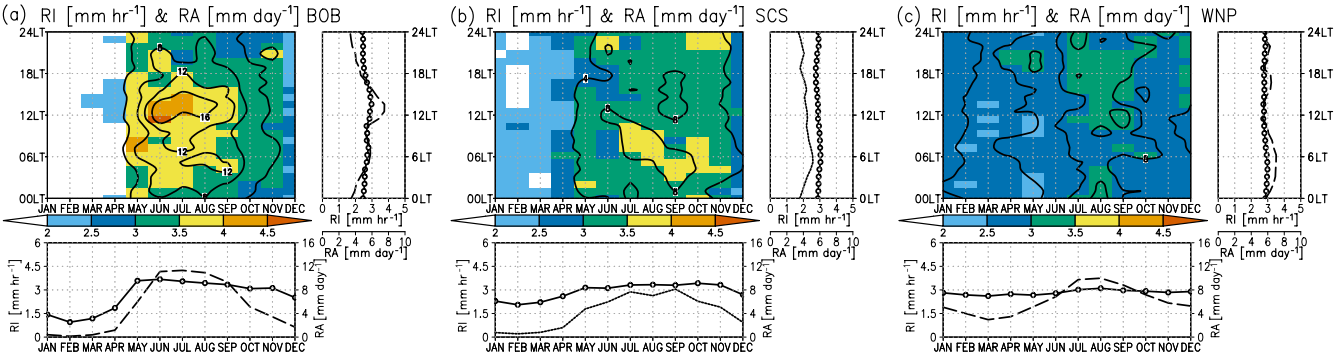

Fig. 5. Same as Fig. 3 but for oceanic regions. The regions are the same as in Fig. 4.

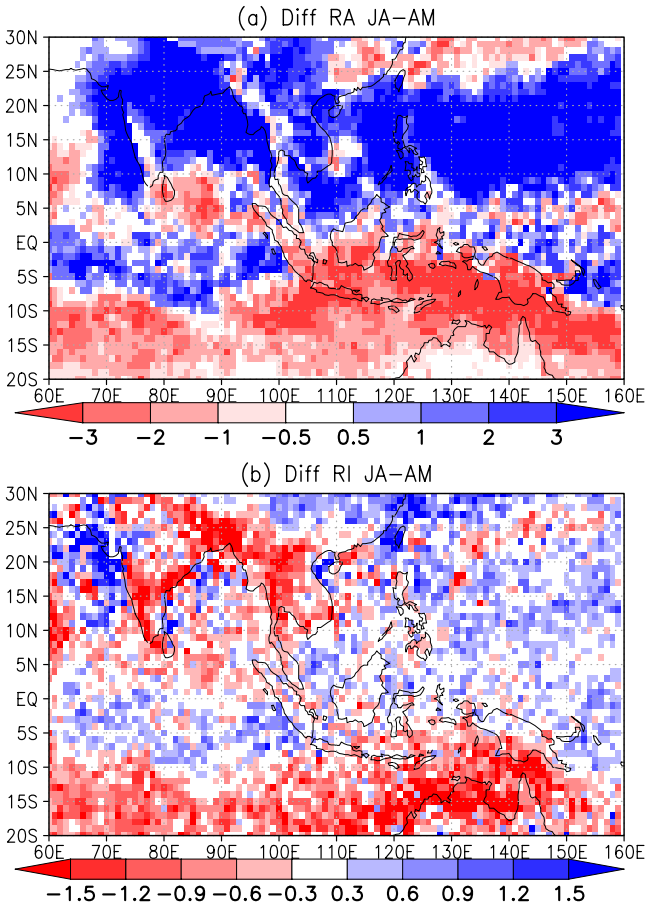

Fig. 6. Spatial distribution of the seasonal difference in (a) RA and (b) RI between April–May and July–August (July–August - April–May). Because June is the onset period of the monsoon season over the ocean, we avoided June for this analysis. A spatial grid scale was converted on a 1° × 1° grid. The unit is mm day^{-1} (mm hour^{-1}) for RA (RI).

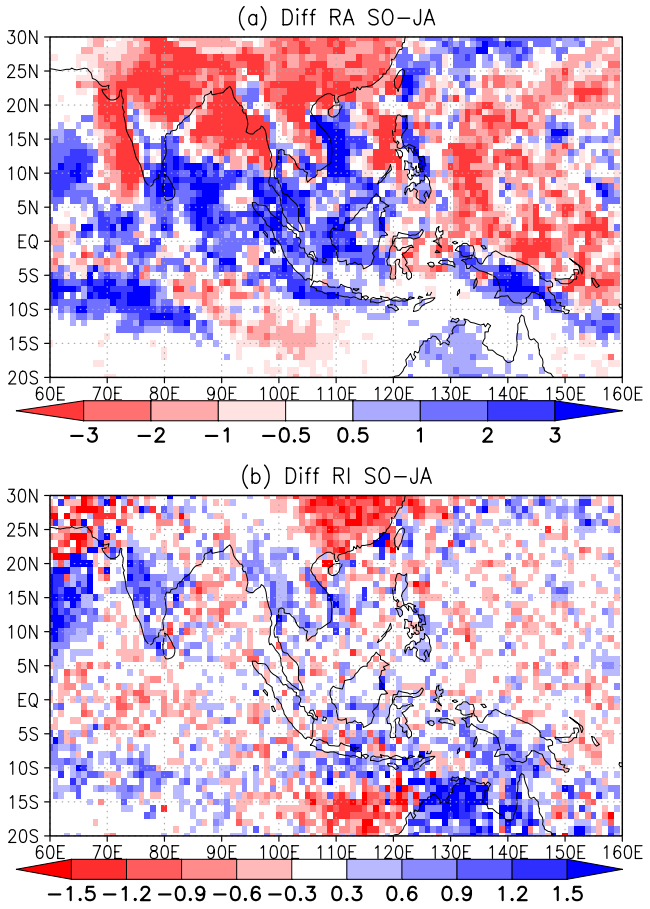

Fig. 7. Same as Fig. 6 but for the difference in (a) RA and (b) RI between July–August and September–October (September–October - July–August).

sonal and diurnal variations of RI over the western North Pacific were very small (Fig. 5c).

Similarly to the seasonal change in RF over the land regions, the RF over the ocean regions had a clear single seasonal peak of RF. Over the ocean, the seasonal variation of RI was much smaller than over the land regions. It was noteworthy that the diurnal variations of RF and RI over the landlocked ocean (the Bay of Bengal) were stronger than over the open ocean (the western North Pacific), which could be an effect of land (e.g., Zuidema 2003).

4. Discussion

4.1 Seasonal change of the spatial pattern of precipitation characteristics

To understand the seasonal change in the spatial pattern of precipitation characteristics, we investigated the changes in precipitation characteristics in terms of meridional displacement of the active precipitation zone, namely the inter-tropical convergence zone (ITCZ). The northward shift of the active precipitation occurred at the onset of the monsoon over the land and ocean regions.

Figure 6 shows that the RI increased from April and May to July and August over almost the entire ocean in the Northern Hemisphere (Arabian Sea, Bay of Bengal, South China Sea, Philippine Sea, and western North Pacific), which is shown in Fig. 5. However, the RI over the Indian Subcontinent, Indochina Peninsula, and Bangladesh Plain decreased from April and May to July and August (Fig. 6b), which is also shown in Fig. 3. Over the ocean, both RA and RI increased with the development of Asian monsoon circulation, while RI decreased over land despite the increase in RA.

In addition, we also showed the seasonal differences in RA and RI between July–August and September–October (Fig. 7). Figure 7 shows almost symmetric seasonal changes in RA and RI from April–May to July–August. Specifically, there was a decrease in RA over the land and ocean north of 10°N, while RI increased over the Indian Subcontinent and the Indochina Peninsula from July–August to September–October. However, an increase in RI over the Bangladesh Plain was not observed. In addition, some differences were found over the Southern Hemisphere.

Based on our results, the differences between the land and ocean in the seasonal change of rainfall characteristics over the tropical Asian monsoon region are summarized in Fig. S1. Figure S1 shows the characteristics of the pre-monsoon season when the equatorial region is in the rainy season. Over land, a stronger RI was observed in the pre-monsoon and post-monsoon seasons of the Asian summer monsoon, which implies that highly convective precipitation systems were dominant. This corresponded to the northern edge of the ITCZ. However, the RF was relatively low over land in the pre-monsoon and post-monsoon seasons. Over the ocean, convective activity was weaker during the pre-monsoon and post-monsoon seasons. During the monsoon season, the RF dramatically increased over land and ocean, in areas that can be under the main body of the ITCZ. Interestingly, the RI weakened over land. However, RI becomes stronger over the ocean. In terms of the diurnal rainfall cycle over land, a low RF with strong RI were observed during daytime in the pre-monsoon and post-monsoon seasons. On the other hand, a high RF with weak/

moderate RI was found during the daytime to early morning in the monsoon season over land.

4.2 Possible mechanism underlying the weakening of RI over land in the wet monsoon season

The previous subsection discussed the weakening of RI over land regions, such as the Indian Subcontinent, Indochina Peninsula, and Bangladesh Plain, from the pre-monsoon to the mature monsoon seasons. The RI over land regions was strengthened in the post-monsoon season. These phenomena were observed only over the land regions, which suggests that the changes of the land-surface conditions could explain these phenomena.

Specifically, the seasonal differences of soil wetness conditions in the period between the monsoon and pre-monsoon/post-monsoon seasons can explain these variations in RI. The wetter soil moisture conditions resulted in a lower surface air temperature as well as a lower height of the planetary boundary layer, which can be explained by the change of the Bowen ratio through the redistribution of absorbed radiation energy at the surface.

A satellite observational study of soil moisture and precipitation in some regions showed that a drier surface induces stronger precipitation particularly over the relatively drier land-surface conditions (Taylor et al. 2012). However, additional studies are needed to determine if their results are in accordance with those in the tropical Asian monsoon regions where the land-surface conditions are relatively wet. In addition, numerical experiments over the wet Asian monsoon regions showed an increase in soil moisture, and a decrease in rainfall amount and RI (e.g., Takahashi et al. 2010b), which may be a regional dependency. Moreover, it is possible that a wetter land surface decreases the height of the planetary boundary layer and weakens local circulations (e.g., Takahashi et al. 2010b), resulting in a weakening of deep convections, although few previous studies have investigated these mechanisms over the wet Asian monsoon regions.

It goes without saying that the seasonal changes of the atmospheric conditions (e.g., Romatschke and Houze 2011a, 2011b; Yamane et al. 2013), such as atmospheric stability, monsoon circulation and moisture transport, can be the primary contributor for the seasonal changes in RI over the land regions. To understand the mechanism of the seasonal changes in RI, additional studies based on observations and modeling are required.

5. Conclusions

This study addressed the seasonal and diurnal variations of precipitation characteristics, namely RA, RF, and RI, over the tropical Asian monsoon region where seasonal changes of climate are dominant. We focused on the difference in seasonal and diurnal variations of precipitation characteristics between land and ocean, using TRMM-PR data over the 15-year period from 1998 to 2012.

Our results demonstrated differences between land and ocean areas in seasonal and diurnal variations in precipitation characteristics. A single seasonal peak in RF was observed over both land and ocean regions. Over land and ocean regions, RF increased with an increase in RA; the increase in RF was explained by an increase in high RF hours. It is noteworthy that daytime precipitation occurred during the relatively drier season, and that nocturnal precipitation often occurred during the relatively wet season over the land regions. Note that double seasonal peaks in RI at the beginning and end of the summer monsoon season were observed over the all land regions, *i.e.*, the two transition seasons (between the wet and dry seasons). This double seasonal peak in RI was not observed over the ocean. In a future study, these rainfall characteristics should be also investigated using widely used rainfall datasets. In addition, convection-permitting numerical experiments are better option to understand the mechanism of seasonal and diurnal rainfall variations over the tropical Asian monsoon region.

Acknowledgments

This work was partly supported by the 7th Japan Aerospace Exploration Agency (JAXA) Precipitation Measuring Mission (PMM) Project No. 306, 8th JAXA PMM Project No. 309 and the "Green Network of Excellence (GRENE)" program of the Ministry of Education, Culture, Sports, Science and Technology, Japan.

Edited by: T. Takemi

Supplement

Supplementary Fig. S1 is a schematic diagram showing the seasonal or spatial pattern changes in precipitation characteristics over the tropical Asian monsoon region, in terms of the different changes between land and ocean. This diagram shows the characteristics of the pre-monsoon season when the equatorial region is in the rainy season.

References

Biasutti, M., S. E. Yuter, C. D. Burleyson, and A. H. Sobel, 2012: Very high resolution rainfall patterns measured by TRMM precipitation radar: Seasonal and diurnal cycles. *Climate Dyn.*, **39**, 239−258.

Fujinami, H., and T. Yasunari, 2001: The seasonal and intraseasonal variability of diurnal cloud activity over the Tibetan Plateau. *J. Meteor. Soc. Japan*, **79**, 1207−1227.

Hirose, M., and K. Nakamura, 2005: Spatial and diurnal variation of precipitation systems over Asia observed by the TRMM precipitation radar. *J. Geophys. Res. Atmos.*, **110**, D05106.

Hirose, M., R. Oki, S. Shimizu, M. Kachi, and T. Higashiuwatoko, 2008: Finescale diurnal rainfall statistics refined from eight years of TRMM PR data. *J. Appl. Meteor. Climatol.*, **47**, 544−561.

Iguchi, T., T. Kozu, J. Kwiatkowski, R. Meneghini, J. Awaka, and K. Okamoto, 2009: Uncertainties in the rain profiling algorithm for the TRMM precipitation radar. *J. Meteor. Soc. Japan*, **87**, 1−30.

Iguchi, T., T. Kozu, R. Meneghini, J. Awaka, and K. Okamoto, 2000: Rain-profiling algorithm for the TRMM precipitation radar. *J. Appl. Meteor.*, **39**, 2038−2052.

Kataoka, A., and T. Satomura, 2005: Numerical simulation on the diurnal variation of precipitation over northeastern Bangladesh: A case study of an active period 14−21 June 1995. *SOLA*, **1**, 205−208.

Kodama, Y.-M., A. Ohta, M. Katsumata, S. Mori, S. Satoh, and H. Ueda, 2005: Seasonal transition of predominant precipitation type and lightning activity over tropical monsoon areas derived from TRMM observations. *Geophys. Res. Lett.*, **32**, L14710.

Ohsawa, T., H. Ueda, T. Hayashi, A. Watanabe, and J. Matsumoto, 2001: Diurnal variations of convective activity and rainfall in tropical Asia. *J. Meteor. Soc. Japan*, **79**, 333−352.

Oki, T., and K. Musiake, 1994: Seasonal change of the diurnal cycle of precipitation over Japan and Malaysia. *J. Appl. Meteor.*, **33**, 1445−1463.

Okumura, K., T. Satomura, T. Oki, and W. Khantiyanan, 2003: Diurnal variation of precipitation by moving mesoscale systems: Radar observations in northern Thailand. *Geophys. Res. Lett.*, **30**, 2073.

Romatschke, U., and R. A. Houze Jr, 2011a: Characteristics of precipitating convective systems in the premonsoon season of South Asia. *J. Hydrometeor.*, **12**, 157−180.

Romatschke, U., and R. A. Houze Jr, 2011b: Characteristics of precipitating convective systems in the South Asian monsoon. *J. Hydrometeor.*, **12**, 3−26.

Romatschke, U., S. Medina, and R. A. Houze Jr, 2010: Regional, seasonal, and diurnal variations of extreme convection in the

South Asian region. *J. Climate*, **23**, 419−439.
Satomura, T., 2000: Diurnal variation of percipitation over the Indo-China Peninsula: Two-dimensional numerical simulation. *J. Meteor. Soc. Japan*, **78**, 461−475.
Satomura, T., K. Yamamoto, B. Sysouphanthavong, and S. Phonevilay, 2011: Diurnal variation of radar echo area in the middle of Indochina. *J. Meteor. Soc. Japan*, **89**, 299−305.
Shimizu, S., R. Oki, T. Tagawa, T. Iguchi, and M. Hirose, 2009: Evaluation of the effects of the orbit boost of the TRMM satellite on PR rain estimates. *J. Meteor. Soc. Japan*, **87**, 83−92.
Stocker, T. F., 2014: *Climate Change 2013: The Physical Science Basis: Working Group I Contribution to the Fifth Assessment Report of the Intergovernmental Panel on Climate Change*. Cambridge University Press, 1552pp.
Takahashi, H. G., 2010: Seasonal changes in diurnal rainfall cycle over and around the Indochina Peninsula observed by TRMM-PR. *Adv. Geosci.*, **25**, 23−28.
Takahashi, H. G., H. Fujinami, T. Yasunari, and J. Matsumoto, 2010a: Diurnal rainfall pattern observed by Tropical Rainfall Measuring Mission Precipitation Radar (TRMM-PR) around the Indochina peninsula. *J. Geophys. Res. Atmos.*, **115**, D07109.
Takahashi, H. G., M. Hara, M. Fujita, and T. Yoshikane, 2012: A discrepancy in precipitable water among reanalyses and the impact of forcing dataset on downscaling in the tropics. *Atmos. Chem. Phys.*, **12**, 23759−23791.
Takahashi, H. G., and T. Yasunari, 2006: A climatological monsoon break in rainfall over Indochina – A singularity in the seasonal march of the Asian summer monsoon. *J. Climate*, **19**, 1545−1556.
Takahashi, H. G., T. Yoshikane, M. Hara, K. Takata, and T. Yasunari, 2010b: High-resolution modelling of the potential impact of land surface conditions on regional climate over Indochina associated with the diurnal precipitation cycle. *Int. J. Climatol.*, **30**, 2004−2020.
Taylor, C. M., R. A. de Jeu, F. Guichard, P. P. Harris, and W. A. Dorigo, 2012: Afternoon rain more likely over drier soils. *Nature*, **489**, 423−426.
Wang, B., 2006: *The Asian Monsoon*. Springer Praxis, 779 pp.
Wang, B., and Z. Fan, 1999: Choice of South Asian summer monsoon indices. *Bull. Amer. Meteor. Soc.*, **80**, 629−638.
Yamane, Y., T. Hayashi, M. Kiguchi, F. Akter, and A. M. Dewan, 2013: Synoptic situations of severe local convective storms during the pre-monsoon season in Bangladesh. *Int. J. Climatol.*, **33**, 725−734.
Zuidema, P., 2003: Convective clouds over the Bay of Bengal. *Mon. Wea. Rev.*, **131**, 780−798.

Manuscript received 9 May 2016, *accepted 12 August 2016*
SOLA: *https://www.jstage.jst.go.jp/browse/sola/*